

Electric Field-induced Charge Transfer of $(\text{Bu}_4\text{N})_2[\text{Ru}(\text{dcbpyH})_2(\text{NCS})_2]$ on Gold, Silver, and Copper Electrode Surfaces Investigated by Means of Surface-enhanced Raman Scattering

Sang-Woo Joo

Department of Chemistry, Soongsil University, Seoul 156-743, Korea. E-mail: sjoo@ssu.ac.kr

Received June 24, 2007

The potential-induced charge transfer of the dye $(\text{Bu}_4\text{N})_2[\text{Ru}(\text{dcbpyH})_2(\text{NCS})_2]$ (N719) on Au, Ag, and Cu electrode surfaces has been examined by surface-enhanced Raman scattering (SERS) in the applied voltage range between 0.0 and -0.8 V. N719 is assumed to have a relatively perpendicular geometry with its bipyridine ring on the metal surfaces. A strong appearance of the carboxylate band at ~ 1370 cm^{-1} indicates that the carboxyl group will likely be deprotonated on the metal surfaces. As the electric potential is shifted from -0.8 to 0.0 V, the $\nu(\text{NCS})$ band at ~ 2100 cm^{-1} on the electrode surfaces appears to undergo a shift in frequency and intensity change. This indicated that the charge transfer between the dye and metal electrode surfaces had occurred. Electric-field-dependent charge transfer differs somewhat depending on the type of metal surfaces as suggested from the dissimilar frequency positions of the $\nu(\text{NCS})$ band.

Key Words : Adsorption, $(\text{Bu}_4\text{N})_2[\text{Ru}(\text{dcbpyH})_2(\text{NCS})_2]$ (N719), Potential-dependent SERS

Introduction

In the past decade, dye-sensitized solar cells have been extensively investigated as a solar-to-electricity conversion system.¹ Ruthenium(II) complexes containing polypyridyl ligands have been widely studied as potential photosensitizers in solar cells.² Metal-to-ligand charge-transfer reactions raise the visible absorption spectra of the dyes and alter their photophysical and redox behavior.³ The functional groups can anchor the dye to the surface and direct the electronic transfer between the donor and the conduction band of the semiconductor.⁴ The ideal dye would have a stable interfacial coupling to the surface as well as optimal optical properties for visible light adsorption.⁵

Numerous techniques have been applied to studying the metal (or semiconductor)/adsorbate interface. Vibrational spectroscopy is one of the most informative tools since it can provide structural information about the chemisorption on the surfaces.⁶ Surface-enhanced Raman scattering (SERS) utilizes another convenient technique used to investigate adsorbates on metal surfaces.⁷ The analysis of spectral features has provided information on adsorption, chemical reactions, and vibrational structures on surfaces.⁸⁻¹⁴

Self-assembly methods represent a unique way to create well-defined nanostructures and thus control surface properties.¹⁵ Characterization of self-assembled monolayers (SAMs) can provide detailed information on the chemical interactions and transformations occurring at surfaces.¹⁶ Although there have been several reports exploring the chemisorption of isothiocyanates on metal surfaces,¹⁷⁻¹⁹ a detailed analysis of the SAMs with their physicochemical characterization has not been well performed yet.

Numerous reports have indicated that adsorption behavior depends on the metal substrates.²⁰⁻²⁷ Recently a density

functional theory study was performed to investigate the adsorption of alkanethiols on Cu, Ag, and Au surfaces, predicting dissimilar ionic characteristics depending on the metal substrates.²⁸ Solvent dependent charge transfer of the ruthenium bipyridine (Ru-bpy) dye on colloidal Ag and Au surface has been recently reported by means of SERS.²⁹ Although quite a few studies have explored the different adsorption structures of SAMs on metal surfaces,²⁰⁻²⁸ no reports have investigated ruthenium bipyridine (Ru-bpy) dye on metal surfaces using potential dependent vibrational spectroscopy.

In this work, the potential-dependent adsorption behavior of N719 on Au, Ag, and Cu electrode surfaces is studied by SERS to better understand the structural change of the adsorbate on surfaces depending on the applied electric field. To the best of the author's knowledge, this is the first comparative potential-dependent adsorption study to employ vibrational spectroscopic tools on different metal electrode surfaces. This work should help elucidate the charge transfer interaction of Ru-bpy on metal surfaces.

Experimental

The dye $(\text{Bu}_4\text{N})_2[\text{Ru}(\text{dcbpyH})_2(\text{NCS})_2]$ (Bu_4N = tetrabutylammonium and dcbpy = dicarboxylbipyridine) N719 (98%) was purchased from Solaronix S.A. (Lausanne, Switzerland) and used without further purification. Figure 1 shows the molecular structure of N719. Raman spectra were obtained using a Renishaw Raman confocal system model 1000 spectrometer equipped with an integral microscope (Leica DM LM). Raman scattering was detected with $180 \times$ geometry using a peltier cooled (-70 °C) CCD camera (400×600 pixels). An appropriate holographic notch filter with the grating (1800 grooves/mm) was set in the spectrometer.

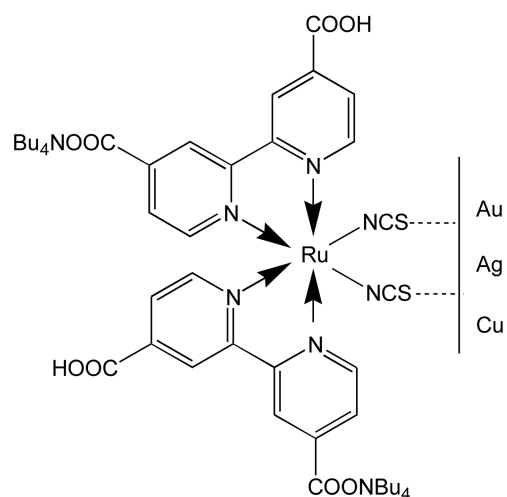


Figure 1. Molecular structure of $(\text{Bu}_4\text{N})_2[\text{Ru}(\text{dcbpyH})_2(\text{NCS})_2]$ (N719) and plausible binding on Au, Ag, and Cu metal surfaces.

The 632.8 nm radiation from a 20 mW air-cooled He-Ne laser (Melles Griot Model 25 LHP 928) with the plasma line rejection filter was used as the excitation sources for the Raman experiments. Data acquisition time used in the Raman measurements was approximately 90 s. The Raman band of the phonon mode in a silicon wafer at 520 cm^{-1} was used to calibrate the spectrometer. After a laser plasma line rejection filter, the Raman scattered light was collected to the detector through a holographic beam splitter. The sample was embedded to a glass capillary (Chase Scientific Glass, Inc) with an outer diameter of 1.1–1.2 mm and ready for the Raman measurement. The laser beam was focused onto a spot approximately $2\ \mu\text{m}$ in diameter with an objective microscope of the order of $\times 20$. The Raman spectrometer was interfaced with an IBM PC and analyzed *via* a Renishaw WiRE software (v. 1.2) based on the GRAMS/32C suite program (Galactic). To further check the electrochemical adsorption behaviors, potential dependent SERS measurements were performed on Au, Ag, and Cu electrode surfaces. An Ag/AgCl electrode was employed as the reference to which all potentials are quoted with respect. A platinum wire was used as the counter electrode. A mini Au, Ag, and Cu working electrode was used and polished with Alumina powder before conducting experiments. The Ag working electrode (part number: CHI 103) and the Au working electrode (part number: CHI 101) from CH instruments and Cu working electrode (catalogue number: 010236) from ALS Co. Ltd. were purchased and used with the outer diameter of 6 mm. Potential dependent measurements between 0 and -0.8 V were obtained using a CH Instruments 700A potentiostat. A homemade Teflon spectroelectrochemical cell was used in an aqueous solution of $\sim 10^{-3}\text{ M}$ N719. The Au SERS substrate was produced from an Au plate by an oxidation-reduction cycle using a potentiostat. The Ag and Cu SERS substrates could be prepared by eroding the Ag and Cu plate using a HNO_3 solution, respectively. Triply distilled water of resistivity greater than $18.0\text{ M}\Omega\text{-cm}$ was used in all experiments without using any

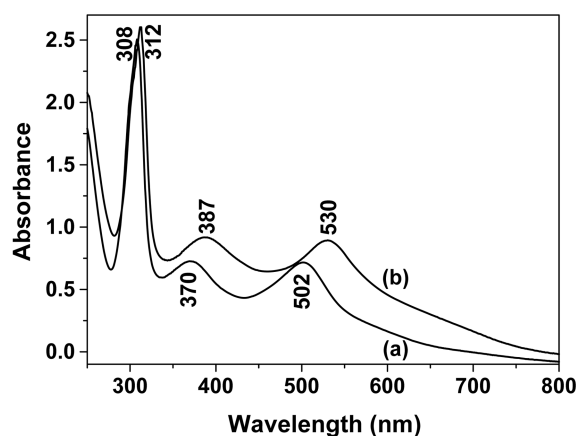


Figure 2. UV-vis absorption spectra ($\sim 10^{-4}\text{ M}$) of N719 in (a) water and (b) ethanol.

electrolytes to avoid introducing any effects from the hydrogen bonding. UV-vis absorbance spectrum was obtained with a Shimadzu 3101-PC UV/VIS/NIR spectrophotometer.

Results and Discussion

UV-vis absorbance spectra of N719. Figure 2 shows the UV-vis absorbance spectrum of N719 in two different solvents of water and ethanol. In the visible region, the spectra of Ru(II) complexes containing polypyridyl ligands are dominated by bands arising from metal-to-ligand charge transfer transitions, in which an electron is promoted from a ruthenium d orbital to the π system of the polypyridyl ligand. The band in the UV region is due to intraligand transitions ($\pi \rightarrow \pi^*$). The bands are strongly solvent dependent and consistent with the previous report.²⁹ The intraligand charge transfer band was observed at 308 nm when the process was performed in water. The metal ligand charge transfer bands were observed at 370 nm and 502 nm. These bands were found at 312, 387, and 530 nm when the process was performed in ethanol.

SERS of N719 on Au, Ag, and Cu electrode surfaces. Figure 3 shows the SERS spectra of $\sim 10^{-3}\text{ M}$ N719 on Au, Ag, and Cu electrode surfaces at a voltage of -0.8 V vs. the standard Ag/AgCl electrode in $900\text{--}2300\text{ cm}^{-1}$. The concentration of N719 in the aqueous solution was $\sim 10^{-3}\text{ M}$ on Au, Ag, and Cu electrode surfaces should correspond to the concentration above a full-coverage limit by assuming that the adsorbate was oriented perpendicularly with respect to the surfaces.

On Au, the vibrational bands at 1605, 1535, 1478, 1427, 1313, 1268, and 1021 cm^{-1} could be ascribed to the bipyridine's ring modes. The two vibrational bands at 1556 and 1373 cm^{-1} can be assigned to the asymmetric and symmetric carboxylate stretching bands, respectively. Along the observation of the carboxylate bands, the absence of the C=O stretching band at 1700 cm^{-1} should indicate that the carboxyl group of N719 should be deprotonated on Au surfaces. The spectral features on Ag and Cu looked rather

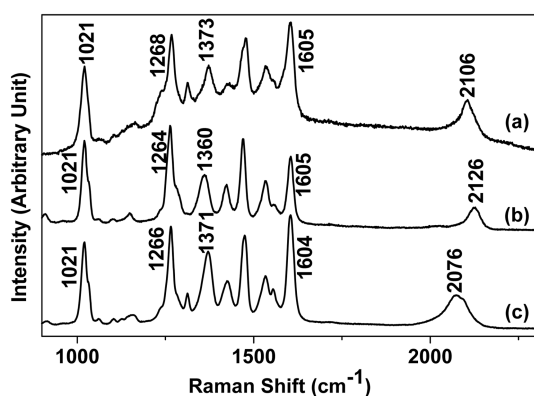


Figure 3. SERS spectra of $\sim 10^{-3}$ M N719 on (a) Au, (b) Ag, and (c) Cu electrode surfaces at a voltage of -0.8 V vs. the standard Ag/AgCl electrode in $900\text{--}2300\text{ cm}^{-1}$. All the spectra were taken by the irradiation light source at 632.8 nm from the HeNe laser.

Table 1. Spectral Data and Vibrational Assignments for N719^a

OR (solid)	Cu (-0.8 V)	Ag (-0.8 V)	Au (-0.8 V)	Assignment ^b
2100	2076	2126	2106	$\nu(\text{NCS})$
1723				$\nu(\text{C=O})$
1609	1604	1605	1605	$\nu(\text{C=C})$ (bpy)
	1556	1558	1556	$\nu_{\text{as}}(\text{COO}^-)$
1545	1534	1535	1535	$\nu(\text{C=C})$ (bpy)
1470	1474	1470	1478	$\nu(\text{C=N})$ (bpy)
1413	1426	1423	1427	$\nu(\text{C=N})$ (bpy)
1364 (IR)	1371	1360	1373	$\nu_s(\text{COO}^-)$
1304	1312		1313	$\nu(\text{C=N})$ (bpy)
1266	1266	1264	1268	$\nu(\text{C=C})$ intern-ring (bpy)
	1021	1021	1021	Ring breathing (bpy)

^aUnit in cm^{-1} . ^bBased on ref. 29.

similar to those on Au. Their peak positions are listed in Table 1 along with the appropriate vibrational assignments. Our assignment is mainly based on the previous literatures.²⁹

Considering that N719 should adsorb on metal surfaces *via* a strong anchoring with the NCS group, the molecule is expected to have a perpendicular orientation. From the electromagnetic (EM) selection rules,³⁰ the vibrational mode perpendicular to the surface should be more enhanced than the parallel one. In our SERS spectra, several strongly observed bipyridine ring modes should be ascribed to the in-plane modes, supporting an upright orientation. This view is consistent with the recent SERS study of N719 on colloidal nanoparticles.²⁹

It is noteworthy that the $\nu(\text{NCS})$ bands are clearly observed at 2106 , 2126 , and 2076 cm^{-1} , on Au, Ag, and Cu, respectively. From the SERS selection rule,³⁰ it was reported that the charge transfer (CT) mechanism could also significantly contribute the enhancement of the SERS intensities. Considering that the bipyridine ring modes looked quite analogous on the three metal surfaces, different frequency positions of the $\nu(\text{NCS})$ bands should indicate a rather dissimilar charge transfer depending on the metal surfaces.

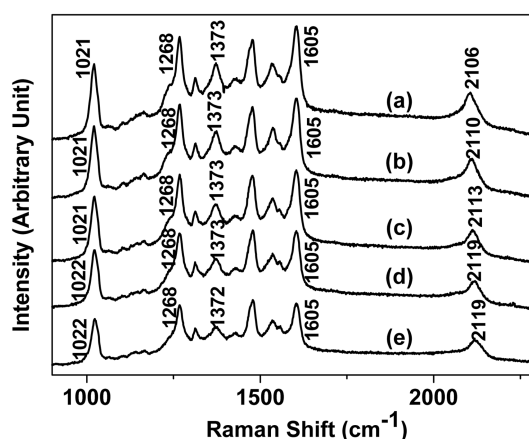


Figure 4. SERS spectra of $\sim 10^{-3}$ M N719 on Au electrode at various voltages of (a) -0.8 , (b) -0.6 , (c) -0.4 , (d) -0.2 , and (e) 0.0 V vs. the standard Ag/AgCl electrode.

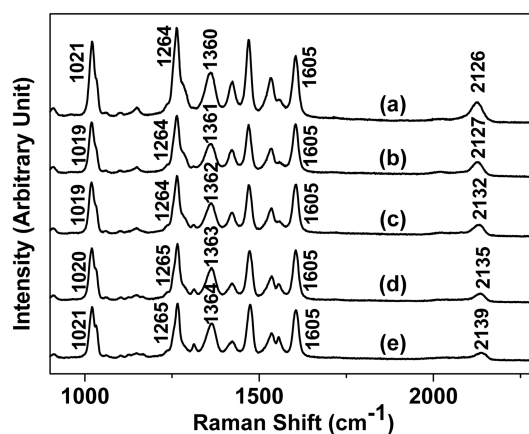


Figure 5. SERS spectra of $\sim 10^{-3}$ M N719 on Ag electrode at various voltages of (a) -0.8 , (b) -0.6 , (c) -0.4 , (d) -0.2 , and (e) 0.0 V vs. the standard Ag/AgCl electrode.

We have conducted electrochemical studies in order to better understand the adsorption characteristics and surface structures of N719 on Au, Ag and Cu electrode surfaces.

Potential-dependent SERS of N719 on Au, Ag, and Cu electrode surfaces. Figures 4, 5, and 6 show the potential-dependent SERS spectra of N719 on Au, Ag and Cu, respectively. It was found that most bipyridine ring bands including the $\nu_s(\text{COO}^-)$ peaks at $\sim 1370\text{ cm}^{-1}$ exhibited less spectral changes in the potential range between -0.8 and 0.0 V. On the other hand the $\nu(\text{NCS})$ vibrational bands showed approximately $\sim 10\text{ cm}^{-1}$ blue-shifts similarly on Au, Ag, and Cu as the potential swept toward to the positive potential by 0.8 V. Their spectra positions depending on the applied voltages are illustrated in Figure 7. Considering that the voltage is quoted with respect to the Ag/AgCl reference electrode, the SERS spectrum at *ca.* -0.2 V should virtually correspond to that in the absence of the electric field. The gradual spectral changes in Figure 7 also supported that the charge transfer should be due to the electric field.

When the potential is more negative, the π^* back donation from the NC bond to the metals can decrease the bond order

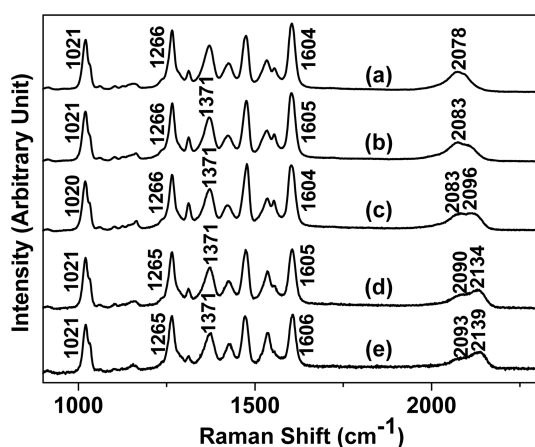


Figure 6. SERS spectra of $\sim 10^{-3}$ M N719 on Cu electrode at various voltages of (a) -0.8 , (b) -0.6 , (c) -0.4 , (d) -0.2 , and (e) 0.0 V vs. the standard Ag/AgCl electrode.

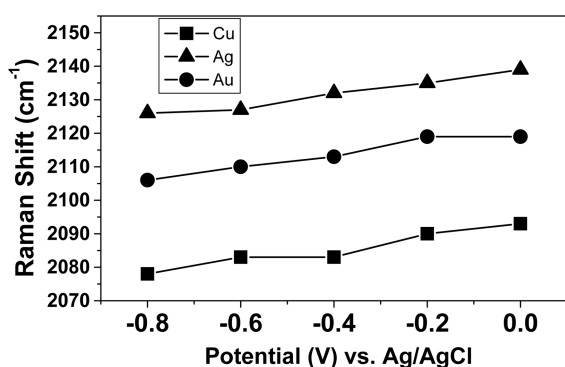


Figure 7. Frequency positions of the NCS stretching modes at ~ 2100 cm^{-1} in the SERS spectra on Cu (\blacksquare), Ag (\blacktriangle), and Au (\bullet) electrode surfaces at various voltages from -0.8 to 0.4 V.

and vibrational frequency. On the other hand, as the potential is made more positive, there is increased σ donation from the C atom to the S atom and the metal, resulting in the increase of the bond order and vibrational frequency due to a shift of electron density from the N atom to the NC bond. The peak intensities of the $\nu(\text{NCS})$ bands were found to change as a function of potential as well. When the potential is more negative, the π^* back donation from the NC bond to the metals can increase in the π -type interaction and the intensity of the $\nu(\text{NCS})$ band.

In the recent dye-sensitized solar cell study³¹ using cyclic voltammetry, an amphiphilic Ruthenium dye [Ru (4,4'-dicarboxylic acid-2,2'-bipyridine) (4,4'-bis(*p*-hexyloxystryl)-2,2'-bipyridine(NCS)₂) which has a similar structure with N719 showed a redox peak at quite a negative voltage of *ca.* -1.0 V on a TiO₂ electrode. For the present study on Au, Ag, and Cu electrodes in the potential range between -0.8 and 0 V, the prominent redox peak could not be observed under our experimental condition.

Intriguingly, the asymmetric $\nu(\text{NCS})$ band became a doublet on the Cu substrate. This may be ascribed to the Fermi resonance that was previously reported.¹⁹ Although not marked in the text, there is a weak peak at ~ 1100 cm^{-1}

due to the pyridine ring vibrations in the Raman spectra. The split band at ~ 2100 cm^{-1} on Cu could be ascribed to the combination band of $\nu_{1021} + \nu_{1100} = \nu_{2121}$ of the pyridine ring vibrations through a Fermi resonance between the $\nu(\text{NCS})$ band and the combination mode.¹⁹ Due to the different $\nu(\text{NCS})$ band positions on Au and Ag, it may not cause a splitting, different from the case of Cu.

Dissimilar charge transfer of N719 on Au, Ag, and Cu may be explained by their different binding energies and bond properties. As predicted from the recent density functional theory calculation of alkanethiols on Ag(111) and Cu(111),²⁸ N719 should have different ionic characteristics and binding energies on Au, Ag and Cu. Due to its intrinsically different bond characteristics, N719 may undergo a dissimilar electron transfer on metal surfaces. This work should facilitate in understanding the adsorption behaviors of ruthenium dye on metal surfaces in the presence of the electric field.

Summary and Conclusions

Electric-field induced charge transfer of N719 on Au, Ag, and Cu surfaces was comparatively examined by means of SERS. On the electrode surfaces, as the potential is swept from -0.8 V to 0.0 V, the $\nu(\text{NCS})$ band at ~ 2100 cm^{-1} became blue-shifted by ~ 10 cm^{-1} , whereas other bipyridine ring modes did not show much deviation. The frequency positions of the $\nu(\text{NCS})$ band appeared to differ depending on the metal surfaces indicating dissimilar charge transfer. In the potential sweep between -0.8 V to 0.0 V, the frequency change of the $\nu(\text{NCS})$ band was similarly observed by ~ 10 cm^{-1} on the metal surfaces.

Acknowledgment. S.W.J would like to thank Prof. Kwan Kim and Prof. Seong Keun Kim for helpful guidance and Mr. Youngmin Kim for helping experiments. This work was supported by the Soongsil University Research Fund.

References

- Grätzel, M. *Nature* **2001**, *414*, 338.
- Hagfeldt, A.; Grätzel, M. *Acc. Chem. Res.* **2000**, *33*, 269.
- Anderson, N. A.; Lian, T. *Annu. Rev. Phys. Chem.* **2005**, *56*, 491.
- Pérez León, C.; Kador, L.; Peng, B.; Thelakkat, M. *J. Phys. Chem. B* **2006**, *110*, 8723.
- Park, H.; Bae, E.; Lee, J.-J.; Park, J.; Choi, W. *J. Phys. Chem. B* **2006**, *110*, 8740.
- Yates, J. T.; Madey, T. E. *Vibrational Spectroscopy of Molecules on Surfaces*; Plenum Press: Plenum, New York, 1987.
- Schatz, G. C.; Van Duyne, R. P. In *Handbook of Vibrational Spectroscopy*; Chalmers, J. M., Griffiths, P. R., Eds.; John Wiley & Sons: New York, 2002; Vol. 1, pp 759-774.
- Kwon, C. K.; Kim, K.; Kim, M. S.; Lee, S.-B. *Bull. Kor. Chem. Soc.* **1989**, *10*, 254.
- Jang, S.; Kim, S. I.; Shin, S.; Joo, S.-W. *Surf. Interf. Anal.* **2004**, *36*, 43.
- Joo, S.-W. *Vib. Spectrosc.* **2004**, *34*, 269.
- Kim, S.; Ihm, K.; Kang, T.-H.; Hwang, S.; Joo, S.-W. *Surf. Interf. Anal.* **2005**, *37*, 294.
- Cho, K.-H.; Choo, J.; Joo, S.-W. *Spectrochim. Acta A* **2005**, *61*, 1141.

13. Yoo, B. K.; Joo, S.-W. *J. Col. Interf. Sci.* **2007**, *311*, 491.
 14. Lim, J. K.; Joo, S.-W. *J. Electroanal. Chem.* **2007**, *605*, 68.
 15. Lehn, J. M. *Supramolecular Chemistry*; Wiley-VCH: Weinheim, 1995.
 16. Ulman, A. *Acc. Chem. Res.* **2001**, *34*, 855.
 17. Ren, B.; Lin, X.-F.; Yang, Z.-L.; Lin, G.-K.; Aroka, R. F.; Mao, B.-W.; Tian, Z.-Q. *J. Am. Chem. Soc.* **2003**, *125*, 9598.
 18. Doering, W. E.; Nie, S. *Anal. Chem.* **2003**, *75*, 6171.
 19. Joo, S.-W. *Surf. Interf. Anal.* **2006**, *38*, 173.
 20. Bae, S. J.; Lee, C.-R.; Choi, I. S.; Hwang, C.-S.; Gong, M.-S.; Kim, K.; Joo, S.-W. *J. Phys. Chem. B* **2002**, *106*, 7076.
 21. Joo, S.-W.; Chung, T. D.; Jang, W.; Gong, M.-S.; Geum, N. H.; Kim, K. *Langmuir* **2002**, *18*, 8813.
 22. Lee, C.-R.; Bae, S. J.; Gong, M.-S.; Kim, K.; Joo, S.-W. *J. Raman Spectrosc.* **2002**, *33*, 429.
 23. Joo, S.-W.; Kim, Y. S. *Col. Surf. A* **2004**, *234*, 117.
 24. Cho, K.-H.; Choo, J.; Joo, S.-W. *J. Mol. Struct.* **2005**, *738*, 9.
 25. Kim, S.; Joo, S.-W. *Vib. Spectrosc.* **2005**, *39*, 74.
 26. Lim, J. K.; Kim, I.-H.; Kim, K.-H.; Shin, K. S.; Kang, W.; Choo, J.; Joo, S.-W. *Chem. Phys.* **2006**, *330*, 245.
 27. Joo, S.-W. *J. Raman Spectrosc.* **2006**, *37*, 1244.
 28. Cometto, F. P.; Paredes-Olivera, P.; Macagno, V. A.; Patrino, E. *M. J. Phys. Chem. B* **2005**, *109*, 21737.
 29. Pérez León, C.; Kador, L.; Peng, B.; Thelakkat, M. *J. Phys. Chem. B* **2005**, *109*, 5783.
 30. Moskovits, M. *Rev. Mod. Phys.* **1985**, *57*, 783.
 31. Zhang, Z.; Zakeeruddin, S. M.; O'Regan, B. C.; Humphry-Baker, R.; Grätzel, M. *J. Phys. Chem. B* **2005**, *109*, 21818.
-